Journal of Fundamental and Applied Research **Vol. 5**, Issue 3 (2025) **20250017**

Received: 13 August 2025 / Accepted: 29 September 2025
Published online: 29 September 2025
© 2025 The Author(s)

Light-induced degeneracies in molecules

Otabek Umarov[1,*] and Islom Egamberdiev[2,†]

[1]*Kimyo International University in Tashkent, Shota Rustaveli street, 156, Tashkent 100121, Uzbekistan*
[2]*Samarkand State Architecture and Construction University named after Mirzo Ulugbek, Lolazor street 70, Samarqand 140143, Uzbekistan*

Abstract. It is well known that LICI can be created by standing or running laser light even in diatomic molecules. The nonadiabatic effect of the formed LICI influences the molecular dynamics. In the present work, we investigate the mechanism of LICI formation and its impact on molecular dynamics under pump-probe laser pulses for the NaH molecule. To obtain molecular nuclear dynamical features, we solve the time-dependent Schrödinger equation (TDSE) for nuclear motion using the multi-configuration time-dependent Hartree (MCTDH) method. The obtained results indicate that the artificial formation of LICIs in the system has a significant impact on the dynamics of the NaH system.

Key words: nonadiabatic effect, light-induced conical intersection, multi-configuration time-dependent Hartree method, classical electromagnetic field.

I. INTRODUCTION

The CI [1–4] has been studied on a large scale in the fields of quantum chemistry and molecular physics research for several decades. This is a common phenomenon in which natural CIs can exist in large quantities in polyatomic molecules. The condition of forming a CI is that a molecular system must have at least two independent nuclear DOF. There is only one vibrational DOF in diatomic molecules; hence, such systems cannot have a natural CI. However, the so-called LICI [5, 6] can be formed in diatomics under the condition that the molecular system is exposed to an external (perturbed) field like quantum or classical light, providing a rotational motion as a second DOF since the inserted external field can rotate the molecular system. In the works [5, 6], the first LICI was theoretically created by both standing and running laser waves. In contrast, the group of Ebbesen [7] carried out the first experimental work, showing that the strong light-matter coupling strength can modify the chemical landscapes of molecular systems.

In the vicinity of natural or light-induced CIs, a conical-shape crossing in energy coordinate with respect to the internuclear coordinate of a molecule emerges, and energy exchange between electronic (even vibrational and rotational) states can take place through this crossing. As a result, in the presence of the CI in the system, the electronic and nuclear motions cannot be treated separately anymore, ending with the breakdown of the BO [3, 8] approximation. Besides, around the degeneracy (or CI) point significant changes in dynamical, spectroscopic [9, 10] and topological properties [11, 12] have been observed in recent decades, giving rise to engaging research topics [12–15] such as Berry phase phenomena, the quantization property of NACs and topological spin etc.

Recent decadal theoretical [5, 6, 16–18] and experimental[7, 19–21] works have shown that chemical landscapes of the molecular systems can be modified and controlled by the light-matter interaction. By changing the laser frequency, the position of LICIs can be determined in the desired energy and internuclear coordinates, allowing for the investigation of different molecular dynamics. If the laser frequency increases, the point of LICIs moves to a larger quantity in both energy and internuclear coordinates, while by changing the laser intensity, the coupling strength between states that the laser couples can be manipulated. The cross-section of NaH transition from the $X^1\Sigma^+$ to $B^1\Pi$ state was investigated in the works [22, 23]. The earlier papers[24] were devoted to studying photon dissociation of the NaH from the ground electronic state $X^1\Sigma^+$ to the repulsive $B^1\Pi$ state via the bound intermediate $A^1\Sigma^+$ state in the pump-probe scheme using the Fourier grid technique in only 1D.

* Corresponding Author: otabekumarov@kiut.uz
† egamberdiyev.islom@samdaqu.edu.uz

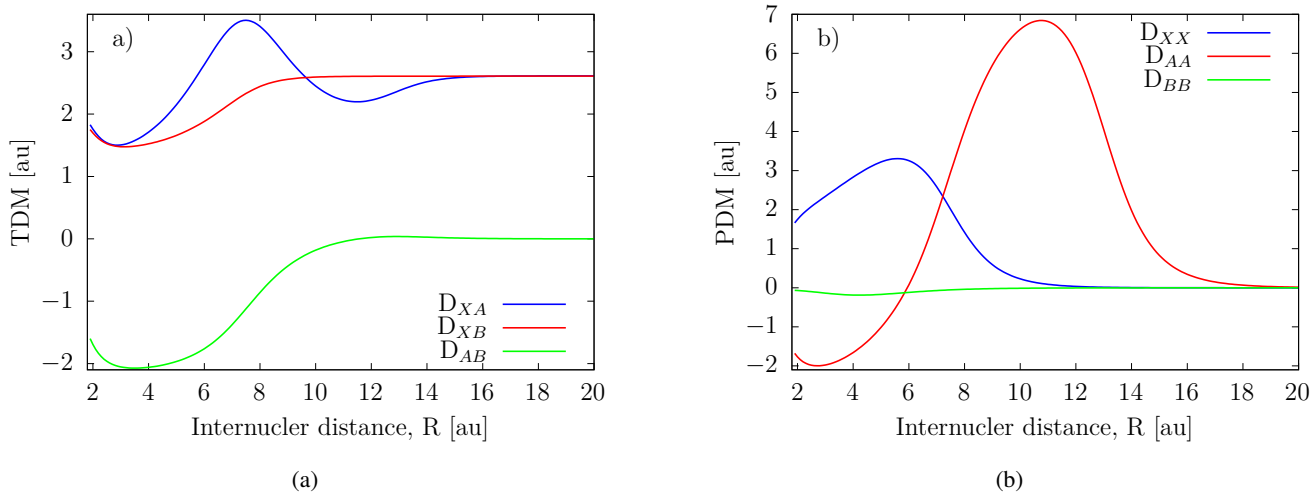
One of the purposes of the current article is to explain the mechanism of the formation of the LICI in the presence of an external field. Another goal of this work is to conduct theoretical simulations of basic molecular dynamical properties of the sodium hydride (NaH) system in the presence of LICIs formed by pump and probe laser pulses.

II. THEORETICAL DESCRIPTION AND METHODOLOGIES

In this section, a brief description of electronic structure calculations for the three singlet electronic states of the NaH system is provided. Furthermore, the three-by-three matrix Hamiltonian and the two laser pulses exposed to the system will be discussed.

A. Ab initio calculations

The earlier works [25–27] had done simulations to obtain the electronic structure calculations; namely, PES, TDM and PDM, for the NaH system with the multiconfiguration self-consistent-field method using one of the accurate and productive ab initio calculations, Molpro[28, 29] quantum package. In Fig. 2, $V_X(R)$, $V_A(R)$, and $V_B(R)$ (solid red, green and blue lines) are the potential energies, while D_{XA}, D_{XB} and D_{AB} in Fig. 1, and D_{XX}, D_{AA}, and D_{BB} in Fig. 1 are the transition and permanent dipole moments of the NaH molecule, respectively.



(a) (b)

FIG. 1: Electronic structure calculations are taken from [25–27], where the Molpro quantum chemistry package (with the aug-cc-pV5Z basis set) in the MRCI method was used. Panels (a) and (b) show the transition and permanent dipole moments of three singlet electronic states of NaH, respectively.

In the region between R=6.3 and 8.9 au, the transition dipole moment between the ground and the first excited states (X-A) is operative (blue line in Fig. 1), whereas the operative region for the TDM of the X-B transition (red line in Fig. 1) corresponds to greater than R=7 au. Although regions corresponding to internuclear distance between R=2.5 to 5.0 au for the A-B TDM (green line in Fig. 1) are effective, about R=7.8 au point plays an important role in the pump-probe scheme we built up, and we will discuss all about it in the subsection II C. It is clear that the PDMs of the ground state between R=2.4 and 7.5 au and the first excited state between R=7 and 14 au are the most operative, whereas the PDM of the second excited state is almost negligible in the entire internuclear distance (see Fig. 1).

B. Wave packet propagation

After the electronic structure calculations have been solved (described in the preceding subsection), we can move to deal with the nuclear dynamics that TDNSE can be used for this purpose, having the form

$$H(R,t)\Psi(R,t) = i\hbar\frac{\partial\Psi}{\partial t} \tag{1}$$

where $\Psi(R,t)$ is the total nuclear wavefunction of the system, and H denotes the working Hamiltonian that includes two terms: the isolated molecular (H_{mol}) and interaction (H_{inter}) part with pump-probe lasers, $H = H_{mol} + H_{inter}$. In case the three

Copyright © 2025

singlet electronic states S_0 ($X^1\Sigma^+$), S_1 ($A^1\Sigma^+$) and S_2 ($B^1\Pi$) of the NaH are considered, the Hamiltonian of the isolated molecular and the interaction terms have the equation 2

$$H = \begin{pmatrix} T_{vib}+T_{rot}+V_X(R) & 0 & 0 \\ 0 & T_{vib}+T_{rot}+V_A(R) & 0 \\ 0 & 0 & T_{vib}+T_{rot}+V_B(R) \end{pmatrix} -$$

$$\begin{pmatrix} D_{XX}(R)[E_{pm}\cos(\theta)+E_{pr}\cos(\theta)] & D_{XA}(R)[E_{pm}\cos(\theta)+E_{pr}\cos(\theta)] & 0 \\ D_{XA}(R)[E_{pm}\cos(\theta)+E_{pr}\cos(\theta)] & D_{AA}(R)[E_{pm}\cos(\theta)+E_{pr}\cos(\theta)] & 0 \\ D_{XB}(R)[E_{pm}\sin(\theta)+E_{pr}\sin(\theta)] & D_{AB}(R)[E_{pm}\sin(\theta)+E_{pr}\sin(\theta)] & 0 \end{pmatrix} -$$

$$\begin{pmatrix} 0 & 0 & D_{XB}(R)[E_{pm}\sin(\theta)+E_{pr}\sin(\theta)] \\ 0 & 0 & D_{AB}(R)[E_{pm}\sin(\theta)+E_{pr}\sin(\theta)] \\ 0 & 0 & D_{BB}(R)[E_{pm}\cos(\theta)+E_{pr}\cos(\theta)] \end{pmatrix} \tag{2}$$

where $T_{vib} = -\frac{1}{2\mu}\frac{\partial^2}{\partial R^2}$ and $T_{rot} = \frac{\partial L^2_{\theta\phi}}{\partial 2\mu R^2}$ are the kinetic energy operators related to vibrational and rotational motions in the molecule, respectively, and R and (θ, ϕ) are the vibrational and rotational coordinates of the molecule, respectively. It is noted that in 1D simulations, the kinetic energy operator that is related to the rotational motion in Eq. 2 is ignored, considering the θ as a constant parameter in the MCTDH calculations, whereas the rotational coordinate is set to the dynamical variable in the 2D model. μ is the reduced mass and $L_{\theta\phi}$ is the angular momentum operator. As mentioned in the previous subsection, $V_X(R)$, $V_A(R)$ and $V_B(R)$ (in Fig. 2) are the potential energies of each singlet electronic state, and D_{XA}, D_{XB}, D_{AB} (in Fig. 1) and D_{XX}, D_{AA}, D_{BB} (in Fig. 1) are the transition and the permanent dipole moments obtained in the Molpro package, respectively. In the interaction Hamiltonian the pump (E_{pm}) and probe (E_{pr}) laser fields are given by

$$\begin{aligned} E_{pm} &= E_{pm_0} f_{pm}(t)\cos(\omega_{pm}t) \\ E_{pr} &= E_{pr_0} f_{pr}(t)\cos(\omega_{pr}t) \end{aligned} \tag{3}$$

where (E_{pm_0}) and (E_{pr_0}) express the peak amplitude of the pump and the probe lasers, and ω_{pm} and ω_{pr} are the laser frequencies of the pump and the probe pulses, respectively. The envelope functions ($f_{pm}(t)$ and $f_{pr}(t)$) have the forms for these lasers

$$\begin{aligned} f_{pm}(t) &= F_{step}\sin^2(\pi(t-t_{pm_0})/t_{pulse_{pm}}) \\ f_{pr}(t) &= F_{step}\sin^2(\pi(t-t_{pr_0})/t_{pulse_{pm}}) \end{aligned} \tag{4}$$

where F_{step} is Heaviside's step function used to confine the laser waves to the desired position, and t_{pm_0}) and (t_{pr_0}) are the starting points of the pump and the probe pulses on the femtosecond (fs) time scale, respectively and their corresponding pulse duration are denoted as $t_{pulse_{pm}}$ and $t_{pulse_{pm}}$.

It is worth noting that the angle θ between the polarization direction of the laser field and the direction of transition dipole moment is perpendicular ($\sin\theta$) in the X-B and the A-B transitions (in Eq. 2) because of the different (Σ and Π) type of symmetries, whereas this angle equals to $\cos\theta$ in the A-B transition (in Eq. 2) due to the same (Σ) type of symmetry (that is, the polarization direction of the laser field and the direction of the A-B transition dipole moment is parallel to each other). The mathematical framework of quantum mechanics relies on the wavefunction, which expresses the essential features of all the information about a quantum system's state. To do so, some basic features of a molecule will be discussed briefly below.

In order to obtain the light-induced electronic transitions between two different electronic states in the system, we use the following Eq. 5 in matrix form

$$d(R) = -\langle\psi_k^{el}(R,\theta,t)|\sum_j r_j|\psi_l^{el}(R,\theta,t)\rangle \tag{5}$$

where $\psi_k^{el}(R,\theta,t)$ is the kth electronic state population, and k,l=1,2,3 ($k \neq l$). The probability of finding a system in a particular state is given by the modulus squared of the wavefunction, $|\psi(R,\theta,t)|^2$. Using the propagated nuclear wave packets, the kth electronic state populations can be obtained as

$$P_k(t) = \left\langle \psi_k^{\mathrm{el}}(R,\theta,t)\middle|\psi_k^{\mathrm{el}}(R,\theta,t)\right\rangle. \tag{6}$$

Atomic units (au)s are used throughout the article; $e = me = \hbar = 1$.

Copyright © 2025

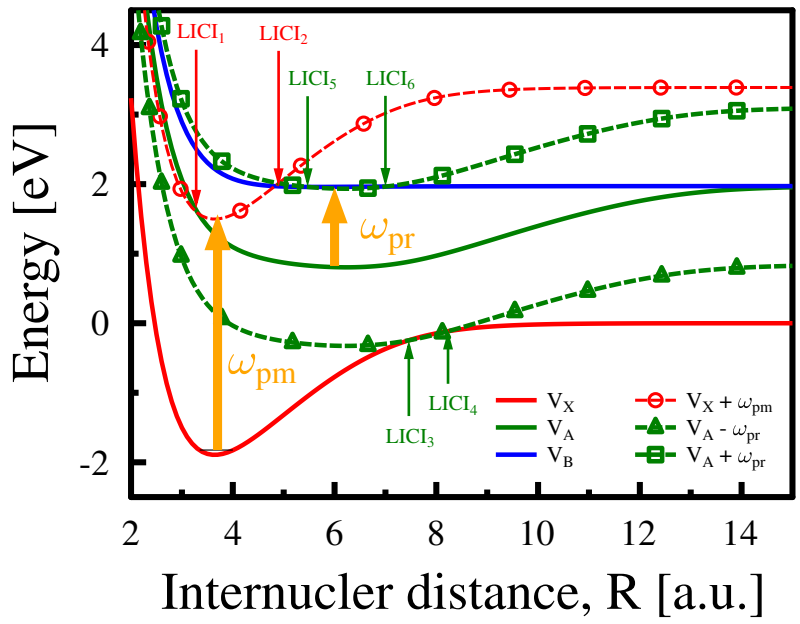


FIG. 2: The pump-probe scheme. The solid red, green and blue curves denote the field-free energies of the ground $X^1\Sigma^+$, the first excited $A^1\Sigma^+$ and the second excited $B^1\Pi$ states, respectively. The red and green dashed curves show the field-dressed states due to the pump (ω_{pm}=3.39 eV), and probe (ω_{pr}=$\omega_{pm}/3$=1.13 eV) pulses, respectively.

C. The pump-probe scheme

The NaH system has been selected to demonstrate the formation of the LICIs between electronic states under the pump and probe pulses. In Fig. 2, the solid red, green and blue curves denote the ground $X^1\Sigma^+$, the first excited $A^1\Sigma^+$ and the second excited $B^1\Pi$ states in turn. The dashed (different-shaped) red and green curves express the field-dressed states due to the applied pump and probe pulses, respectively. The energy of the pump (see the ω_{pm} arrow in Fig. 2) needed to excite the system from the ground state into the first excited one in the vicinity of the FC region is set to 3.39 eV, while the energy of the probe is equal to 1.13 eV in order to couple electronic states.

As the pump pulse is switched on, the $X^1\Sigma^+$ state is shifted upwards (dashed circle-shaped red curve in Fig. 2) by the pump laser energy, ω_{pm}=3.39 eV, and all three electronic states are coupled by this laser pulse. In this case, two light-induced conical intersections (see $LICI_1$ and $LICI_2$ in Fig. 2) between the ground and the first excited electronic states (whenever the two conditions $\cos\theta = 0$ ($\theta = \pi/2$) and $V_A(R) = V_X(R) + \hbar\omega_{pm}$ are simultaneously fulfilled) at around R=3.55 au (energy = 1.353 eV) and between the ground and the second excited electronic states (when the two conditions $\sin\theta = 0$ ($\theta = 0$) and $V_B(R) = V_X(R) + \hbar\omega_{pm}$ are performed at the same time) at nearly R=5.07 au (1.963 eV) are formed. As the second step, as the applied probe pulse is inserted to the system, four extra LICIs: two of them ($LICI_3$ and $LICI_4$) between the ground state and the first excited states at around R=7.5 au (-0.2 eV) and R=8.2 au (-0.1 eV), and two of them ($LICI_5$ and $LICI_6$) between two excited states at around R=4.85 au (1.969 eV) and R=7.47 au (1.966 eV) are built up as $\sin\theta = 0$ and $V_B(R) = V_A(R) + \hbar\omega_{pr}$ are fulfilled.

III. SUMMARY AND CONCLUSION

In conclusion, we have discussed the formation mechanism of the light-induced degeneracies in the presence of the laser fields in the example of the three lowest-lying electronic states of the NaH system. In a molecule interacting with a laser field, the potential energy surfaces of different electronic states can become degenerate as a function of the nuclear coordinates and the laser parameters. Near LICI, the Born-Oppenheimer splitting between electron and nuclear motion becomes invalid in the strong non-adiabatic coupling. Natural and light-induced CIs play a crucial role in non-adiabatic processes, as they serve as efficient funnels for transferring energy from a higher adiabatic surface to a lower one.

Copyright © 2025

REFERENCES

[1] W. Domcke, D. Yarkony, and H. Köppel, *Conical intersections: electronic structure, dynamics & spectroscopy*, Vol. 15 (World Scientific, 2004).
[2] S. Matsika, Reviews in computational chemistry **23**, 83 (2007).
[3] H. Köuppel, W. Domcke, and L. S. Cederbaum, Advances in chemical physics , 59 (1984).
[4] M. Baer, Chemical Physics Letters **35**, 112 (1975).
[5] N. Moiseyev, M. Šindelka, and L. S. Cederbaum, Journal of Physics B: Atomic, Molecular and Optical Physics **41**, 221001 (2008).
[6] M. Šindelka, N. Moiseyev, and L. S. Cederbaum, Journal of Physics B: Atomic, Molecular and Optical Physics **44**, 045603 (2011).
[7] J. A. Hutchison, T. Schwartz, C. Genet, E. Devaux, and T. W. Ebbesen, Angewandte Chemie International Edition **51**, 1592 (2012).
[8] M. Born and W. Heisenberg, Original Scientific Papers Wissenschaftliche Originalarbeiten , 216 (1985).
[9] B. F. Curchod and F. Agostini, The journal of physical chemistry letters **8**, 831 (2017).
[10] C. Xie, B. Zhao, C. L. Malbon, D. R. Yarkony, D. Xie, and H. Guo, The Journal of Physical Chemistry Letters **11**, 191 (2019).
[11] A. F. Izmaylov, J. Li, and L. Joubert-Doriol, Journal of Chemical Theory and Computation **12**, 5278 (2016).
[12] M. V. Berry, Proceedings of the Royal Society of London. A. Mathematical and Physical Sciences **392**, 45 (1984).
[13] H. C. Longuet-Higgins, Proceedings of the Royal Society of London. A. Mathematical and Physical Sciences **344**, 147 (1975).
[14] C. A. Mead and D. G. Truhlar, The Journal of Chemical Physics **70**, 2284 (1979).
[15] I. G. Ryabinkin and A. F. Izmaylov, Physical review letters **111**, 220406 (2013).
[16] J. Galego, F. J. Garcia-Vidal, and J. Feist, Physical Review X **5**, 041022 (2015).
[17] G. Groenhof and J. J. Toppari, The journal of physical chemistry letters **9**, 4848 (2018).
[18] J. Fregoni, G. Granucci, M. Persico, and S. Corni, Chem **6**, 250 (2020).
[19] T. Schwartz, J. A. Hutchison, C. Genet, and T. W. Ebbesen, Physical review letters **106**, 196405 (2011).
[20] A. Thomas, J. George, A. Shalabney, M. Dryzhakov, S. J. Varma, J. Moran, T. Chervy, X. Zhong, E. Devaux, C. Genet, *et al.*, Angewandte Chemie **128**, 11634 (2016).
[21] R. Damari, O. Weinberg, D. Krotkov, N. Demina, K. Akulov, A. Golombek, T. Schwartz, and S. Fleischer, Nature Communications **10**, 3248 (2019).
[22] Q. Guo, J.-W. Hu, J. Qi, J. Yu, and Y.-C. Han, Laser Physics **32**, 045701 (2022).
[23] S. J. Singer, K. F. Freed, and Y. B. Band, The Journal of chemical physics **81**, 3091 (1984).
[24] A. Bhattacharjee and K. R. Dastidar, Journal of Physics B: Atomic, Molecular and Optical Physics **36**, 4467 (2003).
[25] E. S. Sachs, J. Hinze, and N. H. Sabelli, The Journal of Chemical Physics **62**, 3384 (1975).
[26] E. S. Sachs, J. Hinze, and N. H. Sabelli, The Journal of Chemical Physics **62**, 3367 (1975).
[27] W. Zemke, R. Olson, K. Verma, W. Stwalley, and B. Liu, The Journal of chemical physics **80**, 356 (1984).
[28] H.-J. Werner, P. J. Knowles, G. Knizia, F. R. Manby, and M. Schütz, Wiley Interdisciplinary Reviews: Computational Molecular Science **2**, 242 (2012).
[29] K. Shamasundar, G. Knizia, and H.-J. Werner, The Journal of Chemical Physics **135** (2011).

Copyright © 2025

Copyright © 2025